Research Article | Vol. 26, No. 16 | 6 Aug 2018 | OPTICS EXPRESS 20160
Optics EXPRESS

Enhanced-generation of atom-photon entanglement by using FPGA-based feedback protocol

LONG TIAN,[1,2] ZHONGXIAO XU,[1,2] SHUJING LI,[1,2] YAOHUI ZHENG,[1,2,3] YAFEI WEN,[1] AND HAI WANG[1,2,4]

[1]*State Key Laboratory of Quantum Optics and Quantum Optics Devices, Institute of Opto-Electronics, Shanxi University, Taiyuan 030006, China*
[2]*Collaborative Innovation Center of Extreme Optics, Shanxi University, Taiyuan 030006, China*
[3]*yhzheng@sxu.edu.cn*
[4]*wanghai@sxu.edu.cn*

Abstract: The enhanced-generation of entanglement between one atomic collective excitation and a single photon (atom-photon) is very important for practical quantum repeaters and quantum networks based on atomic ensembles and linear optics. We present a feedback-loop algorithm based on field programmable gate array (FPGA) to obtain 21.6-fold increase of the generation rate of atom-photon entanglement at the storage time of 51 μs comparing with no feedback protocol. The generation rate of the atom-photon entanglement is ~3190/s (2100/s) for the excitation probability of 1.65% at the storage time of 1 μs (51 μs). The Bell parameter and the fidelity of atom-photon entanglement at the storage time of 1 μs are 2.40 ± 0.02 and 85.5% ± 0.6%, respectively. The detailed FPGA-based feedback-loop algorithm can be flexibly extended to the multiplexing of atom-photon entanglement, which is expected to further increase the generation rate of atom-photon entanglement.

OCIS codes: (270.0270) Quantum optics; (210.4680) Optical memories; (270.5565) Quantum communications; (270.5585) Quantum information and processing.

References and links

1. L. M. Duan, M. D. Lukin, J. I. Cirac, and P. Zoller, "Long-distance quantum communication with atomic ensembles and linear optics," Nature **414**(6862), 413–418 (2001).
2. N. Sangouard, C. Simon, H. de Riedmatten, and N. Gisin, "Quantum repeaters based on atomic ensembles and linear optics," Rev. Mod. Phys. **83**(1), 33–80 (2011).
3. Z. S. Yuan, Y. A. Chen, B. Zhao, S. Chen, J. Schmiedmayer, and J. W. Pan, "Experimental demonstration of a BDCZ quantum repeater node," Nature **454**(7208), 1098–1101 (2008).
4. N. Gisin, G. Ribordy, W. Tittel, and H. Zbinden, "Quantum cryptography," Rev. Mod. Phys. **74**(1), 145–195 (2002).
5. C. Clausen, I. Usmani, F. Bussières, N. Sangouard, M. Afzelius, H. de Riedmatten, and N. Gisin, "Quantum storage of photonic entanglement in a crystal," Nature **469**(7331), 508–511 (2011).
6. H. Zhang, X. M. Jin, J. Yang, H. N. Dai, S. J. Yang, T. M. Zhao, J. Rui, Y. He, X. Jiang, F. Yang, G. S. Pan, Z. S. Yuan, Y. Deng, Z. B. Chen, X. H. Bao, S. Chen, B. Zhao, and J. W. Pan, "Preparation and storage of frequency-uncorrelated entangled photons from cavity-enhanced spontaneous parametric downconversion," Nat. Photonics **5**(10), 628–632 (2011).
7. D. C. Burnham and D. L. Weinberg, "Observation of simultaneity in parametric production of optical photon pairs," Phys. Rev. Lett. **25**(2), 84–87 (1970).
8. P. G. Kwiat, K. Mattle, H. Weinfurter, A. Zeilinger, A. V. Sergienko, and Y. Shih, "New high-intensity source of polarization-entangled photon pairs," Phys. Rev. Lett. **75**(24), 4337–4341 (1995).
9. P. G. Kwiat, E. Waks, A. G. White, I. Appelbaum, and P. H. Eberhard, "Ultrabright source of polarization-entangled photons," Phys. Rev. A **60**(2), R773–R776 (1999).
10. F. König, E. J. Mason, F. N. C. Wong, and M. A. Albota, "Efficient and spectrally bright source of polarization-entangled photons," Phys. Rev. A **71**(3), 033805 (2005).
11. D. N. Matsukevich, T. Chanelière, M. Bhattacharya, S. Y. Lan, S. D. Jenkins, T. A. Kennedy, and A. Kuzmich, "Entanglement of a photon and a collective atomic excitation," Phys. Rev. Lett. **95**(4), 040405 (2005).
12. D. N. Matsukevich, T. Chanelière, S. D. Jenkins, S. Y. Lan, T. A. Kennedy, and A. Kuzmich, "Entanglement of remote atomic qubits," Phys. Rev. Lett. **96**(3), 030405 (2006).

#331981 https://doi.org/10.1364/OE.26.020160
Journal © 2018 Received 17 May 2018; revised 22 Jun 2018; accepted 23 Jun 2018; published 25 Jul 2018

Optics EXPRESS

13. H. de Riedmatten, J. Laurat, C. W. Chou, E. W. Schomburg, D. Felinto, and H. J. Kimble, "Direct measurement of decoherence for entanglement between a photon and stored atomic excitation," Phys. Rev. Lett. **97**(11), 113603 (2006).
14. S. J. Yang, X. J. Wang, J. Li, J. Rui, X. H. Bao, and J. W. Pan, "Highly retrievable spin-wave-photon entanglement source," Phys. Rev. Lett. **114**(21), 210501 (2015).
15. S. Chen, Y. A. Chen, B. Zhao, Z. S. Yuan, J. Schmiedmayer, and J. W. Pan, "Demonstration of a stable atom-photon entanglement source for quantum repeaters," Phys. Rev. Lett. **99**(18), 180505 (2007).
16. M. Dąbrowski, M. Parniak, and W. Wasilewski, "Einstein-Podolsky-Rosen paradox in a hybrid bipartite system," Optica **4**(2), 272–275 (2017).
17. P. Farrera, G. Heinze, and H. de Riedmatten, "Entanglement between a photonic time-bin qubit and a collective atomic spin excitation," Phys. Rev. Lett. **120**(10), 100501 (2018).
18. R. Ikuta, T. Kobayashi, T. Kawakami, S. Miki, M. Yabuno, T. Yamashita, H. Terai, M. Koashi, T. Mukai, T. Yamamoto, and N. Imoto, "Polarization insensitive frequency conversion for an atom-photon entanglement distribution via a telecom network," Nat. Commun. **9**(1), 1997 (2018).
19. C. Laplane, P. Jobez, J. Etesse, N. Timoney, N. Gisin, and M. Afzelius, "Multiplexed on-demand storage of polarization qubits in a crystalz," New J. Phys. **18**(1), 013006 (2015).
20. C. Xiong, X. Zhang, Z. Liu, M. J. Collins, A. Mahendra, L. G. Helt, M. J. Steel, D. Y. Choi, C. J. Chae, P. H. W. Leong, and B. J. Eggleton, "Active temporal multiplexing of indistinguishable heralded single photons," Nat. Commun. **7**(1), 10853 (2016).
21. O. A. Collins, S. D. Jenkins, A. Kuzmich, and T. A. B. Kennedy, "Multiplexed memory-insensitive quantum repeaters," Phys. Rev. Lett. **98**(6), 060502 (2007).
22. S. Y. Lan, A. G. Radnaev, O. A. Collins, D. N. Matsukevich, T. A. B. Kennedy, and A. Kuzmich, "A multiplexed quantum memory," Opt. Express **17**(16), 13639–13645 (2009).
23. M. Razavi, M. Piani, and N. Lütkenhaus, "Quantum repeaters with imperfect memories: cost and scalability," Phys. Rev. A **80**(3), 032301 (2009).
24. R. Chrapkiewicz, M. Dąbrowski, and W. Wasilewski, "High-capacity angularly multiplexed holographic memory operating at the single-photon level," Phys. Rev. Lett. **118**(6), 063603 (2017).
25. Y. F. Pu, N. Jiang, W. Chang, H. X. Yang, C. Li, and L. M. Duan, "Experimental realization of a multiplexed quantum memory with 225 individually accessible memory cells," Nat. Commun. **8**(1), 15359 (2017).
26. M. Parniak, M. Dąbrowski, M. Mazelanik, A. Leszczyński, M. Lipka, and W. Wasilewski, "Wavevector multiplexed atomic quantum memory via spatially-resolved single-photon detection," Nat. Commun. **8**(1), 2140 (2017).
27. N. Sinclair, E. Saglamyurek, H. Mallahzadeh, J. A. Slater, M. George, R. Ricken, M. P. Hedges, D. Oblak, C. Simon, W. Sohler, and W. Tittel, "Spectral multiplexing for scalable quantum photonics using an atomic frequency comb quantum memory and feed-forward control," Phys. Rev. Lett. **113**(5), 053603 (2014).
28. P. Jobez, N. Timoney, C. Laplane, J. Etesse, A. Ferrier, P. Goldner, N. Gisin, and M. Afzelius, "Towards highly multimode optical quantum memory for quantum repeaters," Phys. Rev. A **93**(3), 032327 (2016).
29. M. Bonarota, J. L. Le Gouët, and T. Chaneliere, "Highly multimode storage in a crystal," New J. Phys. **13**(1), 013013 (2011).
30. D. N. Matsukevich, T. Chanelière, S. D. Jenkins, S. Y. Lan, T. A. B. Kennedy, and A. Kuzmich, "Deterministic single photons via conditional quantum evolution," Phys. Rev. Lett. **97**(1), 013601 (2006).
31. S. Chen, Y. A. Chen, T. Strassel, Z. S. Yuan, B. Zhao, J. Schmiedmayer, and J. W. Pan, "Deterministic and storable single-photon source based on a quantum memory," Phys. Rev. Lett. **97**(17), 173004 (2006).
32. Z. S. Yuan, Y. A. Chen, S. Chen, B. Zhao, M. Koch, T. Strassel, Y. Zhao, G. J. Zhu, J. Schmiedmayer, and J. W. Pan, "Synchronized independent narrow-band single photons and efficient generation of photonic entanglement," Phys. Rev. Lett. **98**(18), 180503 (2007).
33. X. S. Ma, S. Zotter, J. Kofler, T. Jennewein, and A. Zeilinger, "Experimental generation of single photons via active multiplexing," Phys. Rev. A **83**(4), 043814 (2011).
34. L. Tian, Z. Xu, L. Chen, W. Ge, H. Yuan, Y. Wen, S. Wang, S. Li, and H. Wang, "Spatial multiplexing of atom-photon entanglement sources using feedforward control and switching networks," Phys. Rev. Lett. **119**(13), 130505 (2017).
35. M. Mazelanik, M. Dąbrowski, and W. Wasilewski, "Correlation steering in the angularly multimode Raman atomic memory," Opt. Express **24**(19), 21995–22003 (2016).
36. Y. L. Wu, L. Tian, Z. X. Xu, W. Ge, L. R. Chen, S. J. Li, H. X. Yuan, Y. F. Wen, H. Wang, C. D. Xie, and K. C. Peng, "Simultaneous generation of two spin-wave-photon entangled states in an atomic ensemble," Phys. Rev. A **93**(5), 052327 (2016).
37. B. Zhao, Y. A. Chen, X. H. Bao, T. Strassel, C. S. Chuu, X. M. Jin, J. Schmiedmayer, Z. S. Yuan, S. Chen, and J. W. Pan, "A millisecond quantum memory for scalable quantum networks," Nat. Phys. **5**(2), 95–99 (2009).
38. S. J. Yang, X. J. Wang, X. H. Bao, and J. W. Pan, "An efficient quantum light–matter interface with sub-second lifetime," Nat. Photonics **10**(6), 381–384 (2016).
39. Z. Xu, Y. Wu, L. Tian, L. Chen, Z. Zhang, Z. Yan, S. Li, H. Wang, C. Xie, and K. Peng, "Long lifetime and high-fidelity quantum memory of photonic polarization qubit by lifting zeeman degeneracy," Phys. Rev. Lett. **111**(24), 240503 (2013).
40. J. Laurat, H. de Riedmatten, D. Felinto, C. W. Chou, E. W. Schomburg, and H. J. Kimble, "Efficient retrieval of a single excitation stored in an atomic ensemble," Opt. Express **14**(15), 6912–6918 (2006).

Optics EXPRESS

41. M. Sabooni, Q. Li, S. Kröll, and L. Rippe, "Efficient quantum memory using a weakly absorbing sample," Phys. Rev. Lett. **110**(13), 133604 (2013).
42. X. H. Bao, A. Reingruber, P. Dietrich, J. Rui, A. Dück, T. Strassel, L. Li, N. L. Liu, B. Zhao, and J. W. Pan, "Efficient and long-lived quantum memory with cold atoms inside a ring cavity," Nat. Phys. **8**(7), 517–521 (2012).
43. A. G. White, D. F. V. James, P. H. Eberhard, and P. G. Kwiat, "Nonmaximally entangled states: production, characterization, and utilization," Phys. Rev. Lett. **83**(16), 3103–3107 (1999).
44. D. F. V. James, P. G. Kwiat, W. J. Munro, and A. G. White, "Measurement of qubits," Phys. Rev. A **64**(5), 052312 (2001).

1. Introduction

Quantum repeater (QR), which can overcome the distance limit of direct quantum communication, is the basic unit for realizing long-distance quantum communication [1], large-scale quantum network [2,3] and quantum cryptography [4]. The potential of atomic ensembles, serve as quantum memories that is an essential building block for the QR, has recently attracted considerable attention. Motivated by the seminal proposal of Duan, Lukin, Cirac and Zoller (DLCZ), photon-photon entanglement and atom-photon entanglement have been demonstrated from an atomic ensemble. The generation rate of atom-photon entanglement is an important quantity that does not only determine the transfer rate of practical quantum network, but also restrict the maximum distance between two neighboring quantum nodes. To improve the performance of a practical quantum network, one has to increase the generation rate of atom-photon entanglement.

The atom-photon entanglement can be generated by storing one photon from entangled photon pairs, which can be generated through spontaneous parametric down-conversion (SPDC) [7–10], with an in-out quantum memory [5,6]. Spontaneous Raman scattering (SRS) provides a simpler method of generating the atom-photon entanglement [2]. The step is as follows: the atoms firstly interact with the writing light beam in the writing process of SRS, emitting the Stokes photons and creating spin-wave excitations at the same time. The spin-wave excitations are imprinted on the atomic ensemble. After a controllable delay, the spin-wave excitations are mapped into anti-Stokes photons in the reading process of SRS [1]. The scheme spurs intense experimental efforts related to the generation and improvement of the atom-photon entanglement [11–17] via SRS. What is more, these entangled photon pairs can be converted to telecom wavelength by the frequency downconversion process to implement the long-distance quantum communication based on the fiber-optic network [18].

However, limited by the multiexcitations, the generation rate of entangled atom-photon pairs in these experiments has to be kept at a very low level. It is always the key point to enhance the generation rate of atom-photon entanglement without introducing multiexcitation errors. One promising track of current research to increase the generation rate is the experimental implementation of multiplexed interfaces, including temporally multiplexed scheme [19,20], spatially multiplexed scheme [21–26], and spectrally multiplexed scheme [27,28]. Currently, spatially multiplexed quantum memory with more than 665 spatially separated modes is experimental demonstrated [26]. Based on the frequency and temporal multiplexed scheme, researchers have also achieved 500 frequency [27], 400 temporal modes quantum memory [29]. It can be inferred from the current multiplexing capacities that one could simultaneously store 10^8 qubits. These schemes, combining the simultaneous storage of multiple qubits, can enhance the total generation rate of the system on the premise of increasing the generation rate of single mode. The single atom-photon entanglement is building block for constructing the multiplexed interfaces. Here, we wish to increase the generation rate of single atom-photon entanglement to further improve the performance of the multiplexed interfaces.

The feedback circuit has been used to generate the atom-photon entanglement [13], deterministic single photons [30] and increase the generation rate of single-photon source by manipulating the time sequence of the write and read process [31]. Subsequently, the authors implement synchronized generation of two independent single-photon sources from two

Optics EXPRESS

remote atomic ensembles [32]. The two synchronized single-photons are further used to demonstrate efficient generation of entangled photon pairs. Ma et al. demonstrated a fourfold enhancement of the output photon rate by routing four single-photon sources based on the feed-forward technique [33]. However, these feedback loops are limited in these applications, either the enhanced-generation of the single atom-photon entanglement or the router control of multiplexed interfaces.

Recently, our group demonstrates the spatial multiplexing of enhanced-generation of photonic entanglement by using the feedforward control and switching networks [34]. In the spatial multiplexing protocols, multiple Bell-state measurement (BSM) signals acquired from elementary links should be processed and performed as soon as possible. However, there does not mention the construction process of the feedback-loop algorithm.

In this paper, we present a feedback-loop algorithm based on field programmable gate array (FPGA) to realize the enhanced-generation of controllable atom-photon entanglement. The algorithm performs the multi-channel data acquisition and multi-threading parallel process by self-designed program. One of the threads is responsible for the acquisition, storage, judgement, and execution of feedback signal, the other thread performs the buffer reading, coincidence operating, and processed results transferring. The design improves simultaneously the performance of the single atom-photon entanglement source and the router control of multiplexed interfaces. By using the feedback-loop algorithm, we achieve a 21.6-fold increase in generating atom-photon entanglement at the storage time of 51 μs comparing with the non-use of real-time feedback protocol. When the excitation probability is 1.65%, the enhanced generation rate of the atom-photon entanglement pairs is ~3190/s (2100/s), the measured Bell parameter is 2.40 ± 0.02 (2.23 ± 0.12), the fidelity of entanglement state is 85.5% ± 0.6% (83.7% ± 0.8%) at the storage time of 1 μs (51 μs). It is worth of noting that the scheme can be easily extended to the multiplexed atom-photon entanglement [34].

2. Experimental setup and analysis

The experimental setup is illustrated in Fig. 1(a). A cold ^{87}Rb atomic cloud with temperature of about 130 μK is prepared to generate atom-photon entanglement. The size and optical density of atomic cloud are ~5 × 2 × 2 mm^3 and ~7, respectively. After 22.5 ms of loading atoms into the magneto-optical trap (MOT), the cold atoms are first prepared in the initial level $|a\rangle$ by using cleaning beams (C), including a right- (σ^+-) polarized laser beam (tuned on the $|b\rangle \leftrightarrow |e_1\rangle$ transition) and a left- (σ^--) polarized laser beam (tuned on the $|b\rangle \leftrightarrow |e_2\rangle$ transition). The on/off switch for the MOT is controlled by a PXI analog output module (NI PXI-6713). The relevant atomic levels are shown in Fig. 1(b). After the atoms are prepared in the desired state, the σ^+-polarization of write beam (W) goes through the atoms with the waist diameter of 3 mm and is tuned to the transition $|a\rangle \leftrightarrow |e_1\rangle$ with a 20 MHz blue detuning. The cleaning, write and read pulses are manipulated by a feedback protocol switching on/off the operation of three acoustic-optical modulators (AOMs). If we expect to perform the spatially multiplexed scheme, there have two ways of manipulating the switching network, including the usage of more AOMs [34], acousto-optic deflectors (AOD) driven by different modulation frequencies [35]. The Stokes photons are emitted and spin-wave excitations are created at the same time by interacting with the write beam. The spin-wave excitations are stored in the atomic ensemble. After a storage time τ, the σ^--polarization of read beam (R) goes through the atoms with the waist diameter of 3.4 mm and is tuned to the transition $|b\rangle \leftrightarrow |e_2\rangle$. Then, the collective spin-wave excitations are converted into anti-Stokes photons. We call $\{|a\rangle, |b\rangle, |e_1\rangle, |e_2\rangle\}$ the hyperfine levels $\{|5^2S_{1/2}, F=1\rangle, |5^2S_{1/2}, F=2\rangle, |5^2P_{1/2}, F'=1\rangle, |5^2P_{1/2}, F'=2\rangle\}$, respectively. The propagation direction of the read beam is opposite to that of the write beam. The generated Stokes photons and anti-

Optics EXPRESS

Stokes photons are collected by two single-mode optical fiber SMF_S and SMF_{AS}, respectively. Both of the coupling efficiencies of the two fibers are ~80%. We collect Stokes/anti-Stokes photons in the direction that forms a 0.4° angle with the write/read beam.

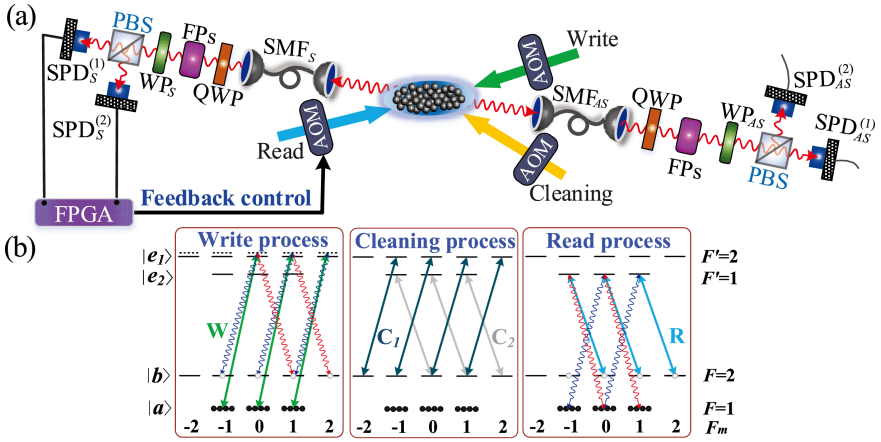

Fig. 1. Overview of the experiment. (a) Illustration of the experimental setup. A read pulse is spatially mode-matched with the write beam from the opposite direction. Both of the Stokes/anti-Stokes photons are collected in single mode fibers and detected by single photon detectors. The on/off switch for the cleaning, write and read pulse is controlled by Field Programmable Gate Array (FPGA). (b) Relevant atomic levels with considering Zeeman sublevels.

The strongly correlated photon pairs and polarization-entangled photon pairs should be generated under the condition of excitation probability $\chi<<1$ [11,36]. In addition, the single-mode fibers, as mode selectors, introduce an extra relative phase difference between the horizontal (H) and vertical (V) polarizations of the optical field, which will degrade the fidelity of entanglement. In order to eliminate the phase-shift difference, a phase compensator (PC) is inserted into the optical path after the output coupler. The phase compensator is a combination of a quarter-wave plate (QWP), a half-wave plate (HWP) and a QWP, which can generate any unitary transformation.

Three 7.5 mm long Fabry-Perot etalons (FPs) are placed after the PC, as filters, to filter out the background noise to a level of 10^{-4} per write/read pulses. The finesse and free spectral range (FSR) of all of the three etalons are 25 and 13.3 GHz. By adjusting the temperature of etalon, optimal transmission can be obtained. The incident angle deviates slightly from the normal incidence on etalon surface to eliminate the parasitic interference. The total transmission of the three etalons is ~80% for the Stokes photons and anti-Stokes photons. A QWP is added in the path of Stokes photons and anti-Stokes photons to transform the σ^+ (σ^-) polarized states of the Stokes photons/anti-Stokes photons into the H (V) polarization. The wave plate (WP_S or WP_{AS}) and polarization beam splitter (PBS), with the extinction ratio of more than 1000:1, are used to perform projection measurement for H-V, D-A [(+45°)-(-45°)] and R-L (σ^+-σ^-) polarization settings. The WP_S and WP_{AS} are half-wave (quarter-wave) plates when analyzing the photon polarization in the D or A (σ^+ or σ^-) polarization setting and are removed when analyzing the photon polarization in H or V polarization setting. In the measurements of the Bell parameter, the WP_S and WP_{AS} are half-wave plates and used for setting the polarization angles. Finally, two couples of single photon detectors (SPD), with multimode fiber coupled input, are adopted to detect the emitted Stokes photons and anti-Stokes photons. The output of the SPD is acquired and analyzed by a FPGA (NI PXIe-7966R). Most importantly, the operation of the FPGA depends on the self-designed, coincidence count and multiplexing program. The generated entangled two-photon state is [11,13]

Optics EXPRESS

$$|\Phi\rangle_{S,AS} = \cos\vartheta|H\rangle_S|H\rangle_{AS} + \sin\vartheta|V\rangle_S|V\rangle_{AS}. \quad (1)$$

where, $\cos\vartheta = \sum p^+_{m_F} / \sum\left(p^+_{m_F} + p^-_{m_F}\right)$ and $\sin\vartheta = \sum p^-_{m_F} / \sum\left(p^+_{m_F} + p^-_{m_F}\right)$. $p^+_{m_F}$ ($p^-_{m_F}$) is the expected distributions of atoms in $|a\rangle$ as a result of σ^+ (σ^-) emission assuming an uniform initial distribution among the various $|b, m_F\rangle$ [11,13].

The time sequence of the experimental cycle is shown in Fig. 2. The duty cycle repeats with a repetition rate of 30 Hz. One duty cycle includes 22.5 ms preparation time, 0.5 ms Sisyphus cooling time and 10 ms operational time. In every operational time, independent write sequences with a period of 1.5 μs are continuously applied to the atomic ensemble until a Stokes photon is detected. Each write sequences contain a cleaning pulse and a write pulse. We retrieve the spin-wave excitations with a fixed delay after a successful write, the spin-wave excitations can be converted into anti-Stokes photons. The pulse width of the cleaning pulse, the write pulse and the read pulse is 250 ns, 80 ns, and 100 ns, respectively. In every write sequences, we release a cleaning pulse with a fixed delay T_1 = 670 ns after a write pulse. The time interval between two neighboring write sequences T_2 is 500 ns. We carry out the next write sequences with a time delay T_2 = 500 ns after a read pulse.

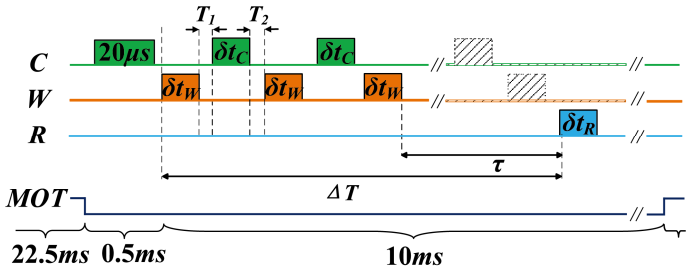

Fig. 2. The time sequence of experimental cycle. A FPGA-based feedback protocol for controlling the cleaning beam, write beam and read beam is used to realize high-speed generation of atom-photon entanglement. The cleaning and write pulses repeat until Stokes photon is detected. The read pulse is only applied conditioned on these events.

The time sequence described above comes true by virtue of a self-designed operation control program, which is stored on FPGA hardware platform. The FPGA manipulates independent AOMs to actuate the on-off action of pulse sequences.

Without feedback protocol, the probability of having a Stokes (an anti-Stokes) photon in one duty cycle is P'_S (P'_{AS}), and that the coincident probability between the Stokes and anti-Stokes channels in one duty cycle is $P'_{S,AS}$. These parameters can be expressed by [31]

$$P'_S = \chi \cdot \eta_S, \quad (2a)$$

$$P'_{AS} = \chi \cdot \eta_{AS} \cdot \gamma, \quad (2b)$$

$$P'_{S,AS} = P'_S \cdot P'_{AS}. \quad (2c)$$

where, χ is the excitation probability, η_S is the total detection efficiency for detecting the Stokes photons, η_{AS} is the total detection efficiency for detecting the anti-Stokes photons and γ is the retrieval efficiency. We don't consider the background noise in each channel.

With feedback protocol, only detecting a stokes photon do we perform the detection of the anti-Stokes photons. So, the probability of having a Stokes (an anti-Stokes) photon P_S (P_{AS}) and the coincident probability between the Stokes and anti-Stokes channels $P_{S,AS}$ should be written as

$$P_S = \chi \cdot \eta_S, \quad (3a)$$

Optics EXPRESS

$$P_{AS} = P_S \cdot \eta_{AS} \cdot \gamma, \tag{3b}$$

$$P_{S,AS} = P_{AS} \tag{3c}$$

We focus on the generation rate of the Stokes (anti-Stokes) photons and the coincidence count in this paper, which are more important for actual quantum commutation. The rate of detected Stokes photons (coincidence count) in the *H-V* polarization setting can evaluate the preparation rate of the atom-photon (photon-photon) entanglement pairs. However, the generation of Stokes photons is probabilistic. The feedback control saves the time of releasing read pulse when the Stokes photon is not detected, which can greatly increase the generate rate of Stokes photon.

With feedback control, the average number of released write pulses N_S and read pulses N_{AS} in one second can be expressed by

$$N_S = \frac{1s}{\left[\chi\left(\delta t_W + \tau + \delta t_R + T_2\right) + \left(1-\chi\right)\left(\delta t_W + T_1 + \delta t_C + T_2\right)\right]}. \tag{4}$$

Then, the generation rate of Stokes photon with feedback control $R^S_{feedback}$ can be expressed by

$$R^S_{feedback} = \frac{P_S \cdot N_S}{1s} = \frac{\chi \cdot \eta_S}{\chi\left(\delta t_W + \tau + \delta t_R + T_2\right) + \left(1-\chi\right)\left(\delta t_W + T_1 + \delta t_C + T_2\right)}. \tag{5}$$

Based on Eqs. (3) and (5), the generation rate of anti-Stokes photon $R^{AS}_{feedback}$ and coincidence count with feedback protocol $R^{S,AS}_{feedback}$ can be expressed by

$$R^{S,AS}_{feedback} = R^{AS}_{feedback} = R^S_{feedback} \cdot \eta_{AS} \cdot \gamma = \frac{\chi \cdot \eta_S \cdot \eta_{AS} \cdot \gamma}{\chi\left(\delta t_W + \tau + \delta t_R + T_2\right) + \left(1-\chi\right)\left(\delta t_W + T_1 + \delta t_C + T_2\right)}. \tag{6}$$

However, in one duty cycle without feedback control, the average number of released write pulses N'_S and read pulses N'_{AS} in one second can be express as

$$N'_S = N'_{AS} = \frac{1s}{\delta t_W + \tau + \delta t_R + T'_1 + \delta t_C + T'_2}. \tag{7}$$

Then, the generation rate of Stokes photon without feedback control $R^S_{non-feedback}$ can be expressed by

$$R^S_{non-feedback} = \frac{P'_S \cdot N'_S}{1s} = \frac{\chi \cdot \eta_S}{\delta t_W + \tau + \delta t_R + T'_1 + \delta t_C + T'_2} \tag{8}$$

Based on Eqs. (2) and (8), the generation rate of anti-Stokes photon $R^{AS}_{non-feedback}$ and coincidence count $R^{S,AS}_{non-feedback}$ without feedback protocol can be expressed by

$$R^{AS}_{non-feedback} = \frac{P'_{AS} \cdot N'_{AS}}{1s} = \frac{\chi \cdot \eta_{AS} \cdot \gamma}{\delta t_W + \tau + \delta t_R + T'_1 + \delta t_C + T'_2}, \tag{9a}$$

$$R^{S,AS}_{non-feedback} = \frac{\chi^2 \cdot \eta_S \cdot \eta_{AS} \cdot \gamma}{\delta t_W + \tau + \delta t_R + T'_1 + \delta t_C + T'_2}. \tag{9b}$$

Optics EXPRESS

where, T_1' is the time interval between write and cleaning pulses; T_2' is the time between read pulse and next cleaning pulse. Without feedback, both the T_1' and T_2' are 150 ns [36]. Based on the Eqs. (5) and (8), the Ratio between $R^S_{feedback}$ and $R^S_{non-feedback}$ is expressed below

$$R^S_{ratio} = \frac{R^S_{feedback}}{R^S_{non-feedback}} = \frac{\chi(\delta t_W + \tau + \delta t_R + T_2) + (1-\chi)(\delta t_W + T_1 + \delta t_C + T_2)}{\delta t_W + \tau + \delta t_R + T_1' + \delta t_C + T_2'}. \quad (10)$$

It should be pointed out that the MOT duration time is not considered in the rate equations [Eqs. (4-10)]. Using these parameters of our atom-photon entanglement generation system (the coupling efficiency of the single-mode fiber 81%; the total transmission of the three etalons 80%; the coupling efficiency of the multimode fiber 95%; the quantum efficiency of the SPD 50%), the generation rate of Stokes/anti-Stokes photons can be theoretically calculated.

3. FPGA implementation of feedback

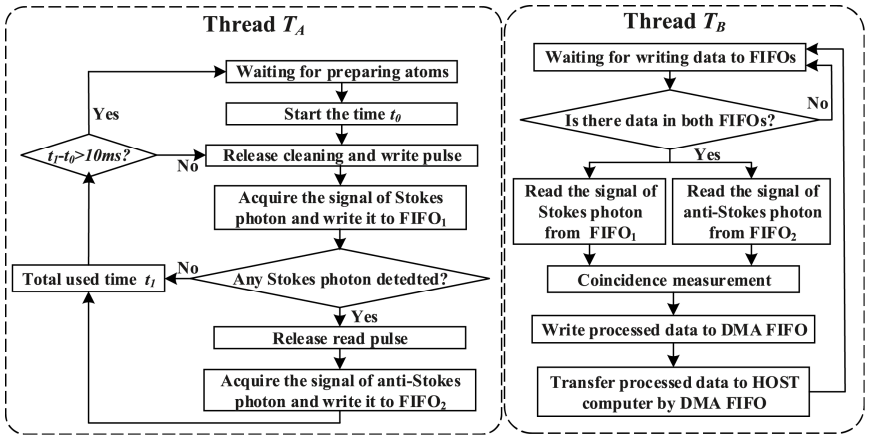

Fig. 3. Block diagram of the FPGA-based feedback-loop algorithm. The acquired signal of Stokes and anti-Stokes photons is written to first-in-first-out (FIFO) buffers in thread T_A, and read from FIFO buffers in thread T_B. The processed data of Stokes photon, anti-Stokes photon and coincidence are transferred to HOST computer by direct memory access (DMA) FIFO buffer.

Single atom-photon entanglement source is an important building block of the experimental implementation of multiplexed interfaces. The enhanced-generation rate of single atom-photon entanglement source is also the core of improving the performance of multiplexed interfaces. The FPGAs, due to the feature of high-speed, scalability and flexibility, become an attractive technique of achieving the feedback-loop algorithm.

Here, Our FPGA-based feedback system hardware composes of NI-PXIe-7966r FPGA module and NI-6581 digital I/O adapter module. The FPGA has 48 input/output channels that can send and receive 48 digital signals at the same time. The system can be extended to 48-fold input/output channels by synchronizing more FPGA modules. So, the FPGA-based feedback system is enough to perform these experiments, such as temporally multiplexed [19,20], spatially multiplexed [22,24,25,34], and spectrally multiplexed interface [27].

The logic programmed onto the FPGA is compiled directly into hardware circuitry. The logic operation is generated by self-designed software program. In order to increase the operation efficiency, we design a multithread parallel data processing scheme to perform the feedback-loop algorithm. The detailed block diagram is shown in Fig. 3. There are two threads T_A and T_B in our FPGA feedback-loop algorithm, running in parallel. The FPGA receives a trigger signal from the analog output module PXI-6713 after the atoms are well prepared and the two threads start to run and last for 10 ms, corresponding to one

Optics EXPRESS

measurement cycle. In the beginning of every measurement cycle, the thread T_A releases the cleaning and write pulse and acquires the signal of Stokes photons. Then, the collected data of Stokes photons is written to a first-in-first-out ($FIFO_1$) buffer. Meanwhile, the thread T_A judges whether a Stokes photon is detected base on acquisition signal. If a Stokes photon is detected, the read pulse will be released and the collected data of anti-Stokes photons will be written to another first-in-first-out ($FIFO_2$) buffer. Otherwise, the read pulse is omitted, the cleaning and write pulse is released again. This can potentially save a lot of time, increase the generated rate. While the thread T_A is still running, the thread T_B runs solely by reading the data stored in the $FIFO_1$ and $FIFO_2$ buffers. The two threads run in parallel, which further save the operation time. The thread T_B consists of judging the buffer status, reading the data from two FIFOs buffer, performing coincidence measurement and writing the results to HOST computer.

4. Experimental results

The excitation probability in our experiment is $\chi \approx 1.65\%$. According to the Eqs. (4) and (6), we calculate the theoretical generation rate of Stokes photon as a function of storage time with feedback protocol (black curve in Fig. 4) and without feedback protocol (red curve in Fig. 4), respectively. These separation points is the experimental results. It can be seen that, from Fig. 4, the generation rate with and without feedback protocol decreases monotonously with the increase of the storage time. Especially for without feedback, the generation rate decreases sharply when the storage time is from 0 to 10 μs, then it is kept at a very low level. While there has small influence of the storage time on the generation rate with feedback protocol. In order to display clearly the explosive growth of the generation rate with feedback protocol, the R_{Ratio}^{S} as a function of storage time is also shown in Fig. 4. At the storage time of 1 μs, 26 μs and 51 μs, the generation rates with feedback protocol are 1.2, 13.3 and 21.6 –fold than those of without feedback protocol, respectively. These results indicate that the generate rate of atom-photon entanglement, in particular for long storage time, can be greatly enhanced by using a real-time FPGA-based feedback protocol.

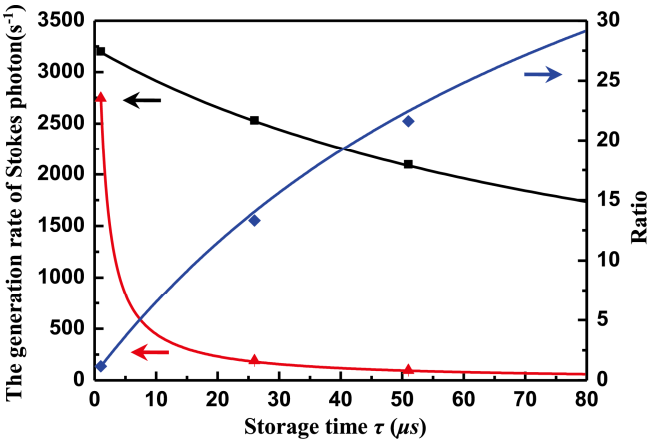

Fig. 4. The generation rates of Stokes photon and ratio R_{Ratio}^{S} as a function of storage time with and without feedback protocol. The solid curves represent the theoretical results; the separation point is the measured results at the storage time of 1 μs, 26 μs and 51 μs.

The total coincidence count rate ($N_{HH} + N_{VV}$) and the retrieval efficiency γ as a function of storage time τ is shown in Fig. 5, N_{HH} (N_{VV}) is the coincidence count rate between detectors $SPD_S^{(1)}$ and $SPD_{AS}^{(1)}$ ($SPD_S^{(2)}$ and $SPD_{AS}^{(2)}$) in the H/V polarization setting. The blue circle (black square) dots are the measured total coincidence count rate (retrieval efficiency) as a

Optics EXPRESS

function of storage time. The red solid curve in Fig. 5 is a fit of the form $\gamma_0 \exp(-\tau^2/\tau_0^2)$ [37] with the lifetime $\tau_0 = 60\ \mu s$ and the initial retrieval efficiency is $\gamma_0 = 15.5\%$ at the storage time of 1 μs. The lifetime can be further improved by applying optical lattice to confine the cold atoms [38] and selecting two pairs of magnetic-insensitive atomic transitions [39].

The retrieval efficiency γ can be calculated by

$$\gamma = \frac{P_{S,AS}}{P_S \cdot \eta_{AS}}. \tag{11}$$

where, $P_{S,AS}$ is coincidence count probability between the Stokes photon and anti-Stokes photon, P_S is the probability of having a Stokes photon, η_{AS} is the total detection efficiency of anti-Stokes photon. According to these parameters, which can be experimentally measured, the retrieval efficiency γ can be calculated and equal to 15.5% at the storage time $\tau = 1\ \mu s$. The retrieval efficiency can be increased by using the high optical-depth cold atoms [40] or coupling the atoms into an optical cavity [41,42].

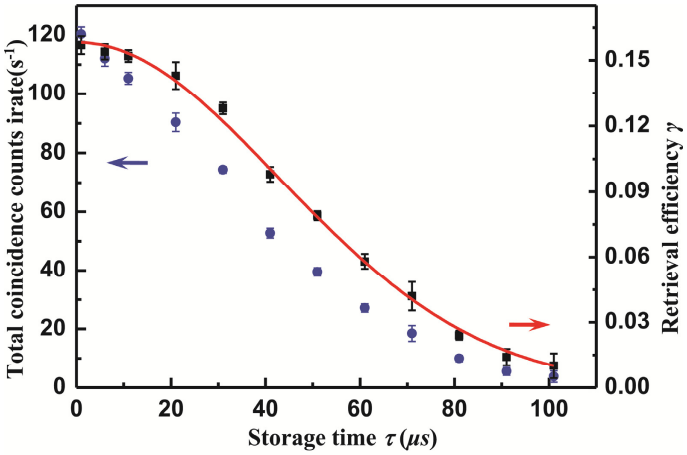

Fig. 5. The total coincidence count rate and the retrieval efficiency γ as a function of storage time τ. The solid curve is a fit of the form $\gamma_0 \exp(-\tau^2/\tau_0^2)$ with $\gamma_0 = 15.5\%$ and $\tau_0 = 60\ \mu s$.

At the storage time of 1 μs, we also measure the polarization ratio (PR) and the total coincidence count rate for the polarization setting of H-V, D-A and R-L as a function of excitation probability χ.

The defining of PRs are

$$PR_{HV(DA)} = N_{//}^{HV(DA)} / N_{\perp}^{HV(DA)}, \tag{12a}$$

$$PR_{RL} = N_{\perp}^{RL} / N_{//}^{RL}. \tag{12b}$$

where, $N_{//}^{HV(DA/RL)} = N_{HH(DD/RR)} + N_{VV(AA/LL)}$ is the coincidence count rate for parallel polarization and $N_{\perp}^{HV(DA/RL)} = N_{HV(DA/RL)} + N_{VH(AD/LR)}$ is the coincidence count rate for perpendicular polarization. For $X/Y = H/V$, D/A or R/L, N_{XX} (N_{YY}) is the coincidence count rate between two detectors $SPD_S^{(1)}$ and $SPD_{AS}^{(1)}$ ($SPD_S^{(2)}$ and $SPD_{AS}^{(2)}$) in X/Y polarization setting, and N_{XY} (N_{YX}) is the coincidence count rate between two detectors $SPD_S^{(1)}$ and $SPD_{AS}^{(2)}$ ($SPD_S^{(2)}$ and $SPD_{AS}^{(1)}$) in X/Y polarization setting.

Figure 6 shows the PRs and total coincidence count rate versus excitation probability χ for polarization setting at H-V, D-A and R-L, respectively. The black squares represent the measured PR, the red circles represent the measured coincidence count rate, the solid line is

Optics EXPRESS

fitting result. The vertical blue dash line across all the plots for $\chi\approx1.65\%$ is drawn in the Fig. 6, which indicates that the PR_{HV} , PR_{DA} and PR_{RL} are 23.8, 8.5 and 8.1 at the $\chi\approx1.65\%$, respectively. The results show that the PR_{HV} is larger than PR_{DA} and PR_{RL}, which can be explained by the non-perfect phase compensation of *SMF*. When increasing the power of the write pulse, the $PR_{HV\ (DA,\ RL)}$ degrade due to the increase of the probability of multiexcitation noise. So it is infeasible to enhance the generation rate of the atom-photon entanglement by increasing largely the power of the write pulse.

Bell parameter of the Bell Clauser-Horne-Shimony-Holt (Bell-CHSH) inequality is used to evaluate the characteristic of atom-photon entanglement. The Bell parameter *S* is defined as

$$S=\left|E\left(\theta_S,\theta_{AS}\right)-E\left(\theta_S,\theta'_{AS}\right)+E\left(\theta'_S,\theta_{AS}\right)+E\left(\theta'_S,\theta'_{AS}\right)\right|. \tag{13}$$

With correlation function $E\left(\theta_S,\theta_{AS}\right)$ given by

$$E\left(\theta_S,\theta_{AS}\right)=\frac{N_{\theta_S,\theta_{AS}}+N_{\theta_S+\pi/2,\theta_{AS}+\pi/2}-N_{\theta_S+\pi/2,\theta_{AS}}-N_{\theta_S,\theta_{AS}+\pi/2}}{N_{\theta_S,\theta_{AS}}+N_{\theta_S+\pi/2,\theta_{AS}+\pi/2}+N_{\theta_S+\pi/2,\theta_{AS}}+N_{\theta_S,\theta_{AS}+\pi/2}}. \tag{14}$$

where θ_S and θ_{AS} are the orientations of polarizers WP_S and WP_{AS}, $N_{\theta_S,\theta_{AS}}$ is the coincidence count rate. For any local realistic theory, the *S* cannot be larger than 2.

Optics EXPRESS

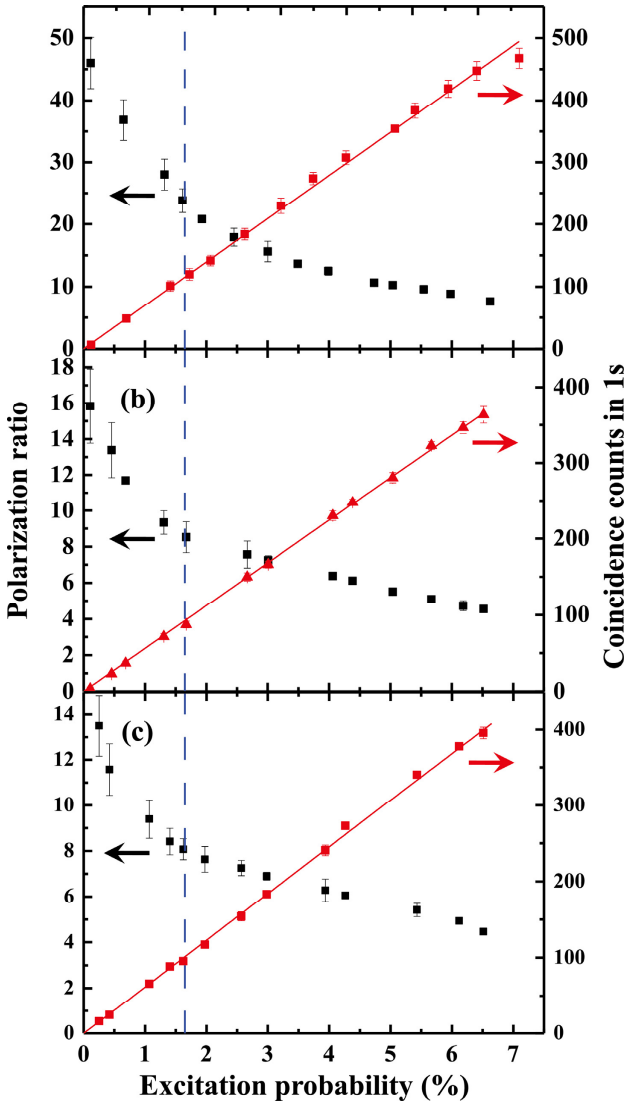

Fig. 6. Polarization ratio and the total coincidence count rate for polarization setting of *H-V* (a), *D-A* (b) and the total coincidence count rate for polarization setting of *R-L* (c) as a function of excitation probability χ at the storage time of 1 *μs*. PR (black squares, left axis), Total coincidence count rate (red circles, right axis), Fitting result (red line, right axis).

The excitation probability χ is fixed to ~1.65% for measuring the Bell parameter. By adjusting the angle of WP_S and WP_{AS}, the $E(\theta_S, \theta_{AS})$ can be measured. A series of orientations of polarizers ($\theta_S = 0$, $\theta'_S = \pi/4$, $\theta_{AS} = \pi/8$, $\theta'_{AS} = 3\pi/8$) is set to obtain the maximum violation for Bell states. As shown in Fig. 7, we obtained $S = 2.40 \pm 0.02$ at the storage time of 1 *μs*, which violates Bell-CHSH inequality by 20 standard deviations. The Bell parameter decreases with the increase of the storage time. At the storage time of $\tau'_0 = 51$ *μs*, the Bell parameter reduces to 2.23 ± 0.12, which confirms the atom-photon entanglement. However, the Bell parameter reduces to 2.00 ± 0.10 at the storage time of 61 *μs* which indicated that the memory is not complete quantum. So, we treat the $\tau'_0 = 51$ *μs* as the memory lifetime of the atom-photon entanglement rather than the fitted lifetime $\tau_0 = 60$ *μs* in Fig. 5. The horizontal line at the level of $S = 2$ is shown in the Fig. 7, which gives the bound of the quantum region.

Optics EXPRESS

The fidelity is calculated by maximum likelihood estimation method, which needs to measure the coincidence count rate of 36 independent projection states [43,44], to further evaluate the generated entanglement state. In this experiment, these projection states are obtained by adjusting the *WPs* placed additionally in front of PBSs. The error bar of fidelity is calculated by Monte-Carlo method.

The calculated density matrix of atom-photon entanglement at the storage time 1 μs is reconstructed as follows:

$$\rho = \begin{pmatrix} 0.6286 & 0.0786+0.0016i & 0.0659+0.0347i & 0.3835+0.0971i \\ 0.0786-0.0016i & 0.0112 & 0.0160+0.0039i & 0.0423+0.0032i \\ 0.0659-0.0347i & 0.0106-0.0039i & 0.0223 & 0.0380-0.0166i \\ 0.3835-0.0971i & 0.0423-0.0032i & 0.0380+0.0166i & 0.3378 \end{pmatrix}. \quad (15)$$

The formula of $F = \left(Tr\sqrt{\sqrt{\rho}\rho_{ideal}\sqrt{\rho}}\right)^2$ is used to calculate the fidelity, where ρ (ρ_{ideal}) is the reconstructed (ideal) density matrices of atom-photon entanglement. The ideally maximum atom-photon entanglement is $|\varphi\rangle = (1/\sqrt{2})(|H\rangle|H\rangle + |V\rangle|V\rangle)$. Based on these formulas and measurement results, the fidelity of atom-photon entanglement is 85.5% ± 0.6% at the storage time of 1 μs.

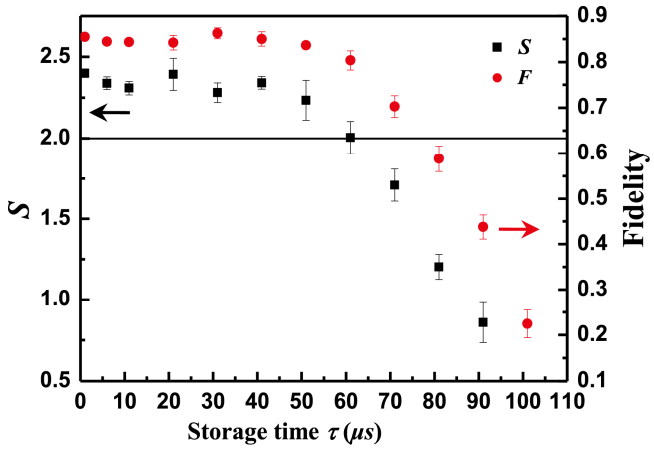

Fig. 7. Bell parameter *S* and fidelity of atom-photon entanglement as a function of storage time τ. Bell parameter *S* (black squares, left axis), Fidelity (red circle, right axis).

In our FPGA feedback system, the FPGA manipulates AOMs and releases ~644000 write pulses and ~3190 read pulse every second for the excitation probability of ~1.65% at the storage time of 1 μs, it has a sampling rate of 100 Mb/s. The data points obtained from every Stokes photon channel is 10.37×10^6 in one second. The feedback signal can be released within ~50 ns after the FPGA acquires multi-channel signals. The FPGA (NI PXIe-7966R) adopted in here has 48 I/O channels, which can obtain maximum 20 ports processing capacity simultaneously. By synchronizing more FPGA modules, it is expected to obtain a significant improvement in the process capacity.

5. Conclusion

In conclusion, we present a feedback-loop algorithm based on FPGA to increase the generation rate of controllable atom-photon entanglement pairs. The algorithm can perform the multi-channel data acquisition and multi-threading parallel process, which can be easily extended to the implementation of multiplexed interface. The multi-channel data acquisition

Optics EXPRESS

and multi-threading parallel data process are realized by the FPGA hardware and self-designed software program, respectively. The program is composed of two threads: One is responsible for judging the buffer status, reading the data from two FIFOs buffer, performing coincidence measurement and writing the results to HOST computer. The feedback protocol does not only increase the generation rate of the single atom-photon entanglement, but also perform conveniently the router control of multiplexed interfaces. By using the feedback-loop algorithm, we achieve a 21.6-fold increase in generating atom-photon entanglement at the storage time of 51 μs comparing with the non-use of real-time feedback protocol. When the excitation probability is 1.65%, the generation rate of the atom-photon entanglement pairs is ~3190/s, the measured Bell parameter is 2.40 with the uncertainty of ± 0.02, the fidelity of entanglement state is 85.5% with the uncertainty of ± 0.6% at the storage time of 1 μs. When the storage time approaches the lifetime (51 μs), the generation rate, Bell parameter and fidelity of entanglement state are 2100/s, 2.23 ± 0.12 and 85.5% ± 0.6%, respectively.

By increasing the retrieval efficiency and lifetime, the generation rate of atom-photon entanglement can be further increased. It is worth noting that the scheme can be easily extended to the multiplexing of atom-photon entanglement, which is expected to further increase the generation rate of atom-photon entanglement.

Funding

National Key Research and Development Program of China (2016YFA0301401); National Natural Science Foundation of China (NSFC) (11475109, 11274211, 11604191, 11654002, 61575114); Program for Sanjin Scholar of Shanxi Province; Fund for Shanxi "1331 Project" Key Subjects Construction.